DOI: 10.61782/fa.2025.0695

FORUM ACUSTICUM EURONOISE 2025

PREDICTION OF IN-DUCT AEROACOUSTIC NOISE OF A MECHANICAL VENTILATION SYSTEM

Ruben D.B. Sevenois[1*]
[1] Vero DUCO, Handelsstraat 19, 8630 Veurne, Belgium

ABSTRACT

The in-duct aeroacoustic sound power of an impeller and volute is predicted up to a frequency of 2.5kHz (approx. 4x the blade passing frequency). The performance of two techniques, compressible LES (LES) and incompressible LES with Perturbed Convective Wave (LES-PCW), are compared. Several volute designs are considered and the accuracy of the prediction is compared to experimental measurements.

Although there is room for improvement, the result show that advanced simulation allows to compare the impact of different volute designs. This allows designers to virtually compare volute designs in a pre-prototype stage. Ultimately, the model can be integrated in a design optimization framework.

Keywords: impeller, volute, aeroacoustic, LES, LES-PCW

1. INTRODUCTION

Increasing awareness for the health hazards associated with continuous sound exposure [1,2] is driving stricter regulations for technical devices in residential buildings. For example, devices with a class A sound performance should emit a sound power lower than 49 dB(A) in technical rooms and 24dB(A) in bedrooms [3].

New and renovated building require a mechanical ventilation system to ensures an excellent indoor air quality. by regulating the humidity and CO_2 level in individual rooms through a system of ducts, valves, a heat exchanger and (radial) impellers. The noise generated by the impellers is propagated through the ducts into people's living spaces. To achieve the desired head pressure, and guide the air flow in the ducting system, the impellers are positioned in a volute. See Figure 1.

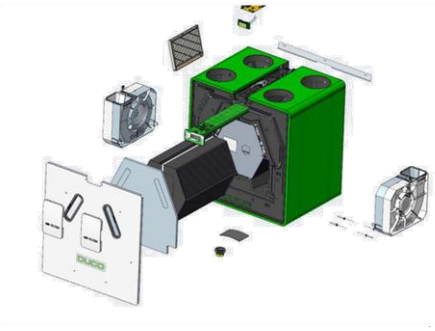

Figure 1. Exploded view of ventilation system.

The interaction of the impeller with the volute structure has a significant impact on the noise footprint. The design of a volute, however, is complex. Many parameters can be tuned and it is not always clear which design features contribute the most. Therefore, advanced simulation methods are investigated to provide insight into the noise generation mechanisms, and perform design optimization.

In this paper the in-duct sound power produced by a radial impeller and volute is predicted using two techniques: 1) Compressible LES (or DNS), and a hybrid method where incompressible LES is combined with a Perturbed Convective Wave (LES-PCW) solver. The simulations are performed with the commercial CFD/CAA software Siemens Simcenter STAR-CCM+ [4]. The performance of both simulation methods are compared amongst each other and to the in-duct sound power measured with a reverberation room. This is done for three volute designs.

[*] ***Corresponding author***: ruben.sevenois@duco.eu

In the following paragraphs first the experimental setup is described. This is followed by a description of the numerical models, with some particularities associated with STAR-CCM+ in Section 3, and the comparison of the performance of the numerical models to the experimental results in Section 4. Section 5 contains the conclusions.

2. EXPERIMENTAL SETUP

Cross sections of the volute designs are shown in Figure 2. The main differences between the designs are indicated by the red markings. Compared to design 190, design 190-1 has an increased tongue radius, and design 190-2 has both a increased tongue radius and increased width of the diffuser. The impeller is a 7-bladed backward curved impeller with a diameter of 190 mm.

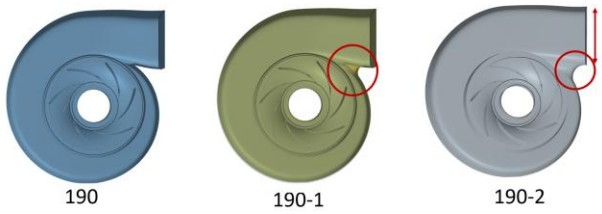

Figure 2. Cross section three volute designs with main differences indicated by red marking.

The in-duct sound power of three different volute designs is measured using a reverberation room in accordance with ISO 5135 [5]. To measure the sound power without influence of the other components of the ventilation system, the volute is placed in a part of the casing. The outlet duct is connected flush with a wall terminating in the space of the reverberation room. This is illustrated in Figure 3.

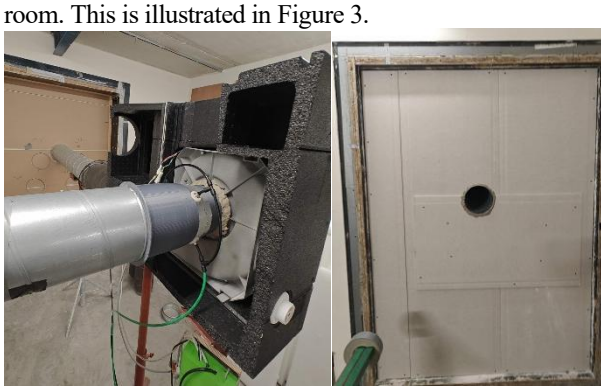

Figure 3. Experimental setup. Volute in part of the casing with outlet connected to reverberation room wall (left) and flush termination of duct (right).

During testing, the impeller is operated at 3900 rpm with an air flow rate of 550 m^3/h. In the reverberation room, a microphone on a rotating boom is swept across the room. The sound power level in the duct in 1/3rd octave bands is calculated by correcting the room sound power with the end-reflection coefficient of the flush termination:

$$L_{Wduct} = L_w + \Delta L_r \tag{2}$$

$$\Delta L_r = 10 \log_{10} \left[1 + \left(\frac{c}{4\pi f} \right)^2 \frac{\Omega}{S} \right] \tag{3}$$

Where L_w is the 1/3rd octave band sound power according to ISO 3741 [6]. c is the speed of sound, f is the 1/3rd octave band mid frequency, Ω is the end termination coefficient (equal to 2π for flush termination) and S is the cross sectional area of the duct. The results of the measurements are discussed in Section 4.

3. NUMERICAL MODEL

Ideally, the simulation model should be as similar as possible to the real experimental setup. This is challenging because the reverberation room has a volume of 214 m^3, about 15000 times the volume of the volute. The mesh requirements for the target frequency range would result in a prohibitive computational cost. Moreover, the reverberant room is treated with sound diffusers and acoustic foams, of which the properties are not known.

3.1 Geometry

Since it not feasible to replicate the experimental setup with an exact digital twin, another approach is applied. Assuming that the duct itself does not produce significant noise, it can be argued that the total sound power is the same at any section between the volute outlet and inside the reverberant room. In other words, the total sound power can also be measured in a section of the outlet duct, provided that it is located sufficiently far from the outlet such that it is not influenced by hydrostatic pressure fluctuations from local turbulence.

Thus, the aeroacoustic model is reduced to the geometry of the impeller with volute, connected with straight ducts extending parallel from the in- and outlets. With the Sound Pressure Level (SPL) from microphones positioned in the in- and outlet duct the sound power can then be calculated. To avoid end-duct reflections, it is important that the end termination of the ducts are non-reflecting. The geometry is shown in Figure 4.

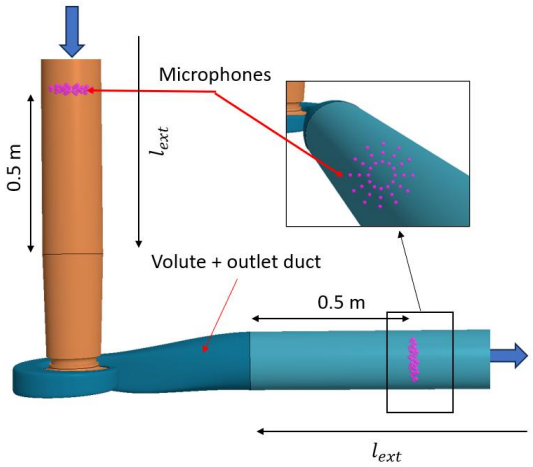

Figure 4. Model geometry and microphone positions

In Figure 4 it can be seen that the in and outlets of the volute are extended with a distance l_{ext}. The length of l_{ext} depends on the model (LES or LES-PCW) applied, see Section 3.3. At a distance of 0.5 m from the in- and outlet a radial array of microphone probes is positioned.

3.2 Mesh

The mesh should be sufficiently small such that both acoustic pressure waves can propagate, and flow features are accurately represented. The mesh is a polyhedral mesh. It was first optimized for flow using a steady state frozen rotor RANS model of the same geometry. The general mesh characteristics are shown in Table 1.

Table 1. General mesh characteristics

Parameter	Value
Base size	2.5 mm
Global min. surface size	0.3 mm
Prism layer thickness	1.5 mm
Nr of prism layers	16
Blade min. surface size	0.16 mm

At the in- and outlet of the volute, the mesh is extruded with the distance l_{ext}. In the extrusions the mesh size gradually increases using a hyperbolic stretching function with initial mesh size 2.5 mm. The increasing numerical dissipation from the gradually increasing size in the extrusions aids to avoid acoustic reflections from the boundary conditions at the in- and outlet.

Next to the general mesh properties, the quality of the interface mesh is tightly controlled. In particular, all cells at each side of the sliding interface should always be connected. Disconnected cells are known to cause divergence, and unphysical spurious acoustic sources. Table 2 contains the settings for the mesh at the interface. The mesh at blade and interface is shown in Figure 5.

Table 2. Interface characteristics

Parameter	Value
Type	Topology
Vertex correction	Close adjacent cells
Surface proximity	Disabled
Prism layers	Disabled
Surface cell type	QUAD

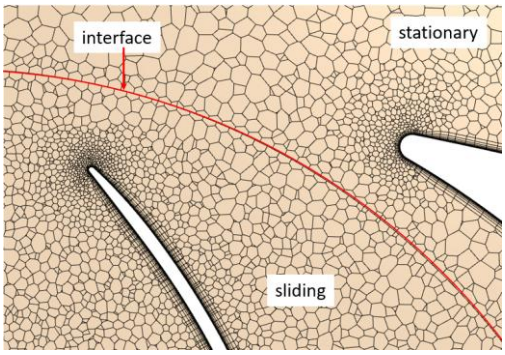

Figure 5. Mesh at interface and blade

Lastly, for acoustic pressure waves, a mesh size smaller than 1/10th of the wavelength of the highest frequency of interest is recommended. For this study, the frequency range of interest is 100 Hz to 2.5 kHz. At standard room conditions, the minimum mesh required for propagating acoustic waves should thus be smaller than 13 mm. Which is, according to Table 1, accommodated to.

3.3 Boundary conditions

A mass flow boundary condition is placed at the inlet. The outlet is a non-reflecting pressure outlet. The walls are modeled as acoustically reflecting, smooth walls.

The usage of the sponge layer governs l_{ext}. For compressible LES a sponge layer is necessary to avoid acoustic reflections from the boundaries. The length of the sponge layer is chosen to be 9m, about 3 times the wave length of the lowest frequency of interest (100 Hz). To ensure that the microphones are outside the sponge layer, l_{ext} is further extended by 1m.

LES-PCW uses an incompressible LES, acoustic wave propagation is thus not explicit modelled and a sponge layer is not required. Therefore l_{ext} can be significantly

smaller for LES-PCW compared to LES. The extrusion distances are given in Table 3.

Table 3. Extrusion lengths

Flow model	l_{ext}
LES	10 m
LES-PCW	1 m

3.4 Flow models and time step

In this paper the performance of two techniques: 1) Compressible LES (or DNS), and a hybrid incompressible LES combined with a Perturbed Convective Wave (LES-PCW) are compared. In the compressible LES the generation and propagation of acoustic waves is integrated by the ideal gas law. The Perturbed Convective Wave (PCW) model is a hybrid acoustics model that uses a wave equation to calculate the sound generation and propagation in incompressible LES. The wave equation solves for an acoustic potential from which the acoustic pressure, -velocity, and -density are derived [4].

The configuration of each model is, for the largest part, identical. Notable differences are that, for LES-PCW a constant density gas law is used (hence incompressible); the time step is larger, and the PCW solver is activated. As mentioned before, the incompressible LES has a sponge layer of 9 m, while the LES-PCW has not. A summary of the configuration is shown in Table 4.

Table 4. Flow models and non-standard solver parameters

	LES	**LES-PCW**
Solver	Coupled Energy, Implicit Unsteady , WALE SGS LES	
Gas	Ideal	Constant Density
Differencing Upwind blend factor	0.15	
Max. inner iterations	15	
Wall treatment	All y+	
Time step [s]	1E-5	5e-5
Time total [s]	0.23	
Acoustic solver	/	Perturbed Convective Wave
Acoustic solver inner iterations	/	10
Sponge layer	9 m	/

For the time step, a convergence study was conducted for each model independently. This resulted in a time step of 1e-5 s for LES, and 5e-5 for LES-PCW. This falls well below the maximum recommended time step half the period of the maximum frequency of interest (2.5 kHz):

$$\Delta t = \frac{1}{2 f_{max}} = 0.0002\ s \tag{4}$$

The simulation is run for a total of 15 rotations of the impeller. This is necessary to let the transient simulation converge to a periodic pattern from the initial state. The initial state of the simulation is the resulting flow, pressure and density field from a steady state frozen rotor RANS. Given that the impeller spins at 3900 rpm, the total time for the simulation is:

$$t_{tot} = \left(\frac{RPM}{60}\right)^{-1} * 15 = 0.23\ s \tag{5}$$

3.5 Computational hardware

All results were obtained on a High Performance Computing cluster with nodes containing 2x 64-core AMD Epyc 7H12 CPUs (“Rome” microarchitecture). A total of 4 nodes, thus 512 cores were used consistently.

3.6 Post-processing

For comparison with the experiment, the SPL of the microphone nodes are post-processed to in-duct sound power in 1/3rd octave bands.

First the SPL at each microphone position is converted to a 1/3rd octave band. Then the average SPL for each duct is calculated from the mean SPL of all microphones for the respective duct (in and outlet). Finally, the total in-duct sound power is calculated from Equation 6.

$$L_W = \overline{L_p} + 10 \log_{10} \frac{S}{S_0} \tag{6}$$

Where $\overline{L_p}$ is the mean sound pressure in the duct, S is the duct cross sectional area and S_0 is a reference area equal to 1 m^2.

For the calculation only the time signal of the pressures (total pressure, acoustic pressure and pressure perturbation) after 4 rotations of the impeller is used. In this way the part of the simulation where the flow has not yet converged, is not taken into account.

4. COMPARISON

In this section the predictions with the several methods are compared against the experimental results obtained for the three geometries (Figure 2). Figure 6 shows a comparison of the prediction by LES and LES-PCW with the experimental results of geometry 190 . Figure 7 shows the comparison of the three geometries experimentally, and simulated with LES-PCW. Table 5 shows the computational effort per method.

As can be seen in Table 5, the computational effort for LES is more than three times higher than for LES-PCW. The amount of cells (even with the increased sponge layer) is approximately the same for each method. The increase in computational effort is mainly due to the smaller time step required for LES.

Table 5. Computational effort

	# [million] cells	Δt [s]	Solve time [h]	CpuH
LES	26.3	1e-5	+144	73 728
LES-PCW	22.9	5e-5	40	20 480

Comparing LES and LES-PCW to the experiments, Figure 6, one can observe that both LES and LES-PCW show the same qualitative trend. Clearly the blade passing frequency, (BPF, about 500Hz) is the dominant frequency. Furthermore, a harmonic of the BPF is visible at 1 kHz in the experiment and in the LES-PCW, but not with LES. Above 2.5 kHz, the power levels with LES drop significantly, while the power of LES-PCW and the experiment stay at a continuous level. Below the BPF a peak can be observed at 63 Hz, which is the rotating rate of the impeller. For the experiment this is logical, as imbalance in the rotor configuration can cause vibrations at the rotating frequency, which might be propagated as sound waves. This is also observed in the simulations, but from a numerical point of view not expected, because the lowest unbalance frequency in load is caused from a blade passing the tongue of the volute. Another possibility is that this peak is numerical noise from the close mismatch between the sliding and stationary mesh, which rematches at every full rotation of the impeller.

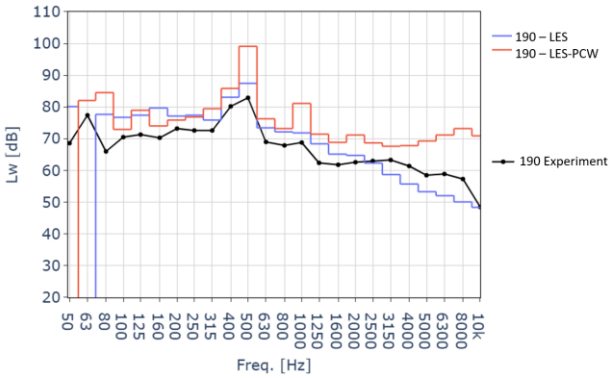

Figure 6. Experimental and predicted in-duct sound power for geometry 190.

Quantitatively, it is clear that LES-PCW severely over-estimates the sound pressure levels. This mainly at the blade passing frequency and its harmonics. The result from LES are closer to the experimental curves, yet still 5dB higher at the BPF.

From previous observation, one could conclude that LES-PCW is not a viable simulation method for the prediction of the sound power of a radial impeller in a volute. Also LES could be seen as not viable. The computational cost is in fact too high for effective application in an industrial environment, where design optimization requires multiple designs to be evaluated fast.

Now, even though the quantitative prediction of the sound power is not accurate, LES-PCW could still be useful in an industrial context (because of the lower computational effort) if the change in sound power level among different designs is similar as observed experimentally.

Figure 7 shows the predictions with LES-PCW and the experimental observations for three different designs. It can be seen that the predicted BPF peak reduces from design 190 to 190-1/190-2 with about the same amount as the experiments. This is also the case for the harmonic peak at 1000 Hz, which almost disappears in design 190-1 and 190-2. Considering that the standard deviation of reproducibility for sound power measurements is between 1.5 dB and 3.0 dB (depending on the one-third octave mid-band frequency) [6], design 190-1 and 190-2 are equivalent. The simulations predict a slightly higher noise level for 190-2.

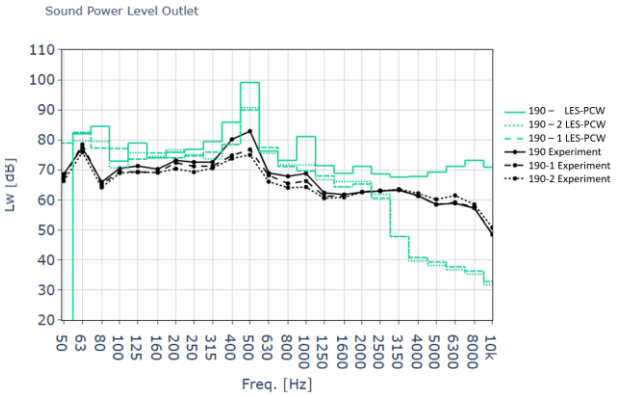

Figure 7. Experimental and predicted in-duct sound power for multiple geometries with LES-PCW

The predicted and experimental total A-weighted sound power levels for the configurations are shown in Figure 8. From the figure it is clear that the simulations follow the same trend as the experiments.

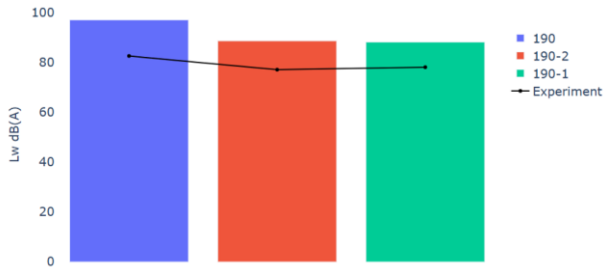

Figure 8. Experimental and predicted in-duct sound power for multiple geometries with LES-PCW

5. CONCLUSIONS

In this work the sound produced by a radial impeller in a volute used in air ventilation systems is predicted using LES and LES-PCW. The performance of both methods are compared to each other, and experimental measurements for three (slightly) different volute geometries.

It is shown that LES requires significantly more computational resources then LES-PCW. This makes LES not suitable for design optimization in an industrial context. The hybrid aeroacoustic method LES with PCW has an acceptable computational cost, but severely overpredicts the measured sound power levels. Qualitatively, however, the same experimental trend can be seen in all simulation results. Including a similar drop in sound pressure level for each 1/3rd octave band frequency.

Although the quantitative predictions are not acceptable, qualitative trends could still be used to perform design optimization. The latter will be the subject of further research.

6. ACKNOWLEDGEMENTS

The resources and services used in this work were provided by the VSC (Flemish Supercomputer Center), funded by the Research Foundation - Flanders (FWO) and the Flemish Government.

Part of this research is funded by VLAIO (Flanders Innovation & Entrepreneurship) in project HBC.2024.0065 .

7. REFERENCES

[1] World Health Organization, Europe. (31/03/2025). *Noise Euro*. https://www.who.int/europe/health-topics/noise#tab=tab_1

[2] European Commission. (31/03/2025). *Noise–European Commission*, https://environment.ec.europa.eu/topics/noise_en

[3] Windey Jos, Vinçotte.(2020) *Geluidscomfort in residentiële gebouwen, welke wijzigingen voor 2020?*

[4] Siemens Digital Industries Software. (2024). *Simcenter STAR-CCM+ 2410 User Guide*

[5] International Organization for Standardization. (1997). *Acoustics - Determination of sound power levels of noise from air-terminal devices, air-terminal units, dampers and valves by measurement in a reverberation room (ISO 5135:1997,IDT)*

[6] International Organization for Standardization. (2009). *Acoustics - Determination of sound power levels and sound energy levels of noise sources using sound pressure - Precision methods for reverberation test rooms (ISO 3741:2010,IDT)*